# Evidence for a short spin diffusion length in permalloy from the giant magnetoresistance of multilayered nanowires

S. Dubois and L. Piraux
*Unité de Physico-Chimie et de Physique des Matériaux, Place Croix du Sud 1, B-1348 Louvain-la-Neuve, Belgium*

J. M. George
*Unité Mixte de Recherche Thomson/CNRS, LCR Thomson, F-91404 Orsay, France and Université Paris–Sud, Bâtiment 510, F-91405 Orsay, France*

K. Ounadjela
*Institut de Physique et Chimie des Matériaux de Strasbourg, F-67037 Strasbourg, France*

J. L. Duvail
*Unité de Physico-Chimie et de Physique des Matériaux, Place Croix du Sud 1, B-1348 Louvain-la-Neuve, Belgium*

A. Fert
*Unité Mixte de Recherche Thomson/CNRS, LCR Thomson, F-91404 Orsay, France and Université Paris–Sud, Bâtiment 510, F-91405 Orsay, France*

(Received 15 December 1997; revised manuscript received 3 April 1998)

We present magnetization and giant magnetoresistance (GMR) measurements performed on two series of electrodeposited $Py$/Cu multilayered nanowires ($Py = Ni_{80}Fe_{20}$) of diameter $\phi = 90$ nm. The multilayers of the first series are composed of a conventional stacking of *Py* and Cu layers and the GMR is studied as a function of the Cu thickness for a constant *Py* thickness. The multilayers of the second series are composed of $Py$/Cu/$Py$ trilayers uniformly distributed along the filament and separated from each other by thick Cu layers. For this second series, magnetic and GMR properties were investigated as a function of the *Py* layer thickness and our magnetization measurements demonstrate that, for *Py* layers thinner than about 90 nm, the magnetic moments of the two *Py* layers of a trilayer are approximately antiparallel at zero field. Analysis of the GMR data using the Valet-Fert model allows us to estimate that the spin diffusion length in *Py*, $\ell_{sf}^{(Py)}$, is between 3.3 and 5.3 nm. [S0163-1829(99)06125-1]

## I. INTRODUCTION

Electrodeposition into nanometer-sized pores of a template polymer membrane has recently proved to be a reliable method to fabricate arrays of magnetic nanowires with interesting magnetic and transport properties.[1–3] More precisely, the simplicity of this method to fabricate multilayered structures and the extremely large aspect ratios that can be obtained, make such arrays of multilayered nanowires ideally suited for the investigation of the giant magnetoresistance (GMR) with the current perpendicular to the planes of the layers (CPP geometry). This approach to CPP-GMR experiments is certainly simpler than those based on superconducting contacts and ultrasensitive superconducting quantum interference device (SQUID)-based systems, or pillar-shaped microstructures.[4–6] A first interest of the CPP geometry compared to the current in the plane of the layers (CIP) geometry comes from the larger magnetoresistance ratios obtained in the former for similar layer thicknesses and identical materials.[7,8] As an example, GMR ratios ($\Delta R/R^P$) up to 80% were obtained at low temperature on $Py$/Cu multilayered nanowires[8] with 12-nm-thick *Py* layers and 4-nm-thick Cu layers. The GMR ratio we measured on this multilayered nanowires array is at least larger by a factor of 20 than the values reported for $Py$/Cu multilayers in the CIP geometry[9,10] for similar layer thicknesses. The different scaling of the CIP and CPP-GMR comes from the existence, in the latter, of spin relaxation and spin accumulation effects due to spin transport through the interface. As stressed by the Valet-Fert (VF) model,[11] the scaling length of the CPP problem is the relatively long spin diffusion length (SDL) whereas the scaling length of the CIP problem is the much shorter electron mean free path. In the so-called long SDL limit, that is when the SDL is much thicker than the individual layer thicknesses, the magnetoresistance does not depend on the SDL and is given, in the framework of the VF model, by simple expressions[11] already derived from a two current series-resistor approach.[12] The predicted behavior in this limit has been confirmed by extensive sets of experimental data obtained on different systems.[5,7,13,14] The SDL, an important parameter in spin injection devices,[15] can be determined only from measurements on samples where the layer thicknesses are thicker than the SDL. For ferromagnetic layers, the SDL has been determined only for Co and permalloy. As stressed in our previous works,[16] the main difficulty for determining the SDL comes from the uncertainty on the magnetic arrangement in the resistance maximum state. For Co/Cu nanowires, the proportion of antiparallel arrangement of the magnetization in consecutive layers has been derived directly from magnetic force microscopy experiments and

 

used in the analysis of GMR data to derive the SDL in Co (59 nm at 77 K).[17] For permalloy, the SDL has been derived by Steenwyk *et al.*[18] from measurements on spin valve structures in which an antiparallel arrangement is obtained by pinning one of the *Py* layers with FeMn. A value of 5 nm is found at 4.2 K. This is surprisingly short, especially if we compare it with the SDL in the micron range found by Johnson.[15] It was of clear interest to settle this discrepancy.

In this paper, we report on the determination of the SDL in *Py* in electrodeposited *Py*/Cu multilayered nanowires. The paper is divided as follows. The sample preparation is described in Sec. II. In Sec. III, we recall theoretical expressions for the CPP-GMR variation, both in the long SDL limit and in the small SDL limit, and derive expressions for the trilayer-based systems [structure schematically depicted in Fig. 1(b)]. In Sec. IV, we analyze the results of GMR in conventional multilayered nanowires composed of a periodic stacking of *Py* and Cu. We next discuss, in Sec. V, magnetization and GMR data on a series of trilayer-based samples. From the analysis of the data, we extract the SDL in *Py*. Finally, we present a discussion of the SDL value in *Py* in Sec. VI and our conclusions in Sec. VII.

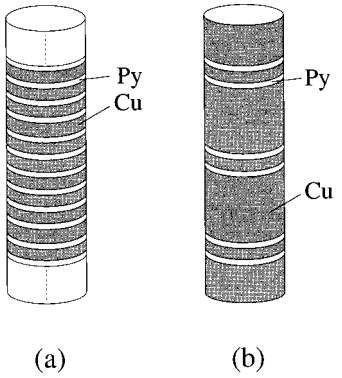


FIG. 1. Schematic representation of the different multilayered structures investigated in this work.

## II. SAMPLE PREPARATION

Track-etched polycarbonate membranes were used as nanoporous host material.[19] The average pore diameter and pore length were 90 nm and 20 $\mu$m, respectively. The cross section is uniform along the pore length except over a distance of 100–200 nm from the extremities where the diameter is slightly reduced. The roughness and size distribution of the pores are also reduced compared to commercially available porous membranes.[19,20] Electrodeposited $Ni_{80}Fe_{20}(Py)$/Cu multilayered nanowires were made at room temperature from a single sulfate bath containing $Ni^{2+}$, $Fe^{2+}$, and $Cu^{2+}$ ions by using a pulsed electrodeposition technique as described in Ref. 8. The structure and chemical composition of the nanowires have been characterized by transmission electron microscopy (TEM) and energy dispersive spectroscopy of x rays (EDX).[8,21] The nanowires can be separated into polycrystalline and monocrystalline regions. The single crystals extend over more than one hundred of periods. Large GMR ratios also confirm that our multilayered nanowires are of fairly good quality.

## III. THEORETICAL BACKGROUND FOR CPP-GMR

### A. Conventional *F*/*N* multilayers

By conventional multilayers, we mean the structure shown in Fig. 1(a), with a periodic stacking of magnetic and nonmagnetic layers. We call $t_N$ ($t_F$) and $\ell_{sf}^{(N)}$ ($\ell_{sf}^{(F)}$) the thickness and spin diffusion length (SDL) of the nonmagnetic (ferromagnetic) layers. In the long SDL limit, that is for $t_N \ll \ell_{sf}^{(N)}$, $t_F \ll \ell_{sf}^{(F)}$, and in the absence of spin mixing[22] at temperatures much smaller than the Curie temperature, the VF model[11] predicts simple expressions of the CPP-GMR that are equivalent to those derived by a phenomenological resistor series model.[12] There are several ways of writing down these expressions; for example,

$$\left(\frac{\Delta R}{R^{\mathrm{AP}}}\right)^{-1/2} = \frac{\rho_F^* t_F + 2r_b^*}{\beta\rho_F^* t_F + 2\gamma r_b^*} + \frac{\rho_N^* t_N}{\beta\rho_F^* t_F + 2\gamma r_b^*} \qquad (1)$$

with $\Delta R = R^{\mathrm{AP}} - R^{\mathrm{P}}$. We use the same notations as in Ref. 11, i.e., $\rho_{\uparrow(\downarrow)} = 2\rho_N^*$, $\rho_{\uparrow(\downarrow)} = 2\rho_F^*[1-(+)\beta]$ for the resistivity of the nonmagnetic and magnetic layers, respectively, and $r_{\uparrow(\downarrow)} = 2r_b^*[1-(+)\gamma]$ for the interface resistance. $\beta$ and $\gamma$ are the bulk and interfacial spin asymmetry coefficients, respectively. Although, in the initial VF model,[11] expressions of the type of Eq. (1) had been derived in the simple case where $R^{\mathrm{P}}$ and $R^{\mathrm{AP}}$ are the resistances of parallel and antiparallel configurations, it can be shown[23] that the resistance $R^{\mathrm{AP}}$ is the same for a strict antiparallel arrangement and when, less drastically, AP refers to a state with zero mean magnetization for a set of magnetic layers included within a total thickness range of the order of the SDL (the equivalence of antiparallel and random configurations has also been demonstrated in Ref. 24 in the simple case of infinite SDL).

### B. Structures composed of *F*/*N*/*F* trilayers separated by thick layers of *N*

We consider the structure represented in Fig. 1(b) where $F/N/F$ trilayers are separated by very thick layers of a nonmagnetic metal $N$. Our notation for the thicknesses is $t_F$ for the magnetic layers, $t_{N1}$ for the thin nonmagnetic layer inside a trilayer, and $t_{N2}$ for the thick nonmagnetic spacer. A straightforward extension of the VF model[11] to the geometry of Fig. 1(b) (with also the additional assumption $t_{N1} \ll t_{N2}$, $t_F$, $\ell_{sf}^{(N)}$, and $t_{N2} > \ell_{sf}^{(N)}$ corresponding to our experiments) leads to the following general expression of the resistance per period in the AP and P configurations:

$$R^{\mathrm{AP}}=R_0+4\beta\gamma r_b^*+2\,\frac{[2\cdot\beta^2 r_F(r_N+r_b^*)-2\beta\gamma r_b^* r_F]\left[ch\left(\frac{t_F}{\ell_{sf}^{(F)}}\right)-1\right]+[\beta^2+r_F^2-\gamma^2(r_b^*)^2]sh\left(\frac{t_F}{\ell_{sf}^{(F)}}\right)}{r_F ch\left(\frac{t_F}{\ell_{sf}^{(F)}}\right)+(r_N+r_b^*)sh\left(\frac{t_F}{\ell_{sf}^{(F)}}\right)},$$

$$R^{\mathrm{P}}=R_0+2\,\frac{\left\{\beta r_F sh\left(\frac{t_F}{\ell_{sf}^{(F)}}\right)+\gamma r_b^*\left[ch\left(\frac{t_F}{\ell_{sf}^{(F)}}\right)+1\right]\right\}\cdot[\beta r_N+2(\beta-\gamma)r_b^*]}{(r_b^*+r_N)ch\left(\frac{t_F}{\ell_{sf}^{(F)}}\right)+r_F sh\left(\frac{t_F}{\ell_{sf}^{(F)}}\right)+r_b^*}, \tag{2}$$

where $r_N=\rho_N^*\cdot\ell_{sf}^{(N)}$, $r_F=\rho_F^*\cdot\ell_{sf}^{(F)}$, $R_0=\rho_N^* t_{N2}+2(1-\beta^2)\rho_F^* t_F+4(1-\gamma\beta)r_b^*$. Actually, as we see in the next sections, these trilayered structures are specifically designed to study the regime $t_F\gg\ell_{sf}^{(F)}$. With the additional assumption $r_F\gg r_b^*$, $r_N$, one derives from Eq. (2) the following relatively simple equation for this regime:

$$\frac{\Delta R}{R^{\mathrm{P}}}=\frac{\beta^2}{(1-\beta^2)}\cdot\frac{\ell_{sf}^{(F)}}{t_F}. \tag{3}$$

The physics of Eq. (3) is simple. Referring to Fig. 2, the only difference from the current distribution between the AP configuration of Fig. 2(a) and the P configuration of Fig. 2(b) is within a depth of approximate thickness $\ell_{sf}^{(F)}$ in the magnetic layers on both sides of the central nonmagnetic layer. In the AP configuration, the spin ↑ and spin ↓ currents are approximately equal in a central region of thickness $2\ell_{sf}^{(F)}$ and the resistance of this central region is approximately $2\rho_F^*\ell_{sf}^{(F)}$. In the P configuration, the asymmetry between the spin ↑ and spin ↓ currents is the same as in the bulk ferromagnetic material and the resistance of the central region is $2(1-\beta^2)\rho_F^*\ell_{sf}^{(F)}$. This leads to $\Delta R=2\beta^2\rho_F^*\ell_{sf}^{(F)}$ and with $R^{\mathrm{P}}=2(1-\beta^2)\rho_F^* t_F$, one obtains Eq. (3). We also see that with $t_F\gg\ell_{sf}^{(F)}$, the current distribution and the GMR are controlled only by the magnetic configuration of the two magnetic layers inside a trilayer. Each trilayer contributes independently to the GMR, by $\Delta R=2\beta^2\rho_F^*\ell_{sf}^{(F)}$ if its configuration is AF, by zero for a P configuration. Consequently, Eq. (3) can be extended straightforwardly to the case with a proportion $p$ of AP trilayers:

$$\frac{\Delta R}{R^{\mathrm{P}}}=p\cdot\frac{\beta^2\cdot\ell_{sf}^{(F)}}{(1-\beta^2)t_F}. \tag{4}$$

Thus in the limit we have considered, the MR ratio is independent of $t_{N1}$ and $t_{N2}$, and is proportional to $p$, $\ell_{sf}^{(F)}$ and $1/t_F$. We also note that $\Delta R/R^{\mathrm{P}}$ is half what is calculated for conventional $F/N$ multilayers in the limit $t_F\gg\ell_{sf}^{(F)}$, $t_N\ll\ell_{sf}^{(N)}$.[17]

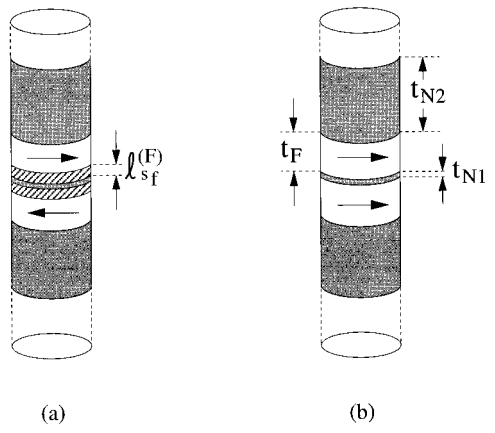


FIG. 2. Schematic representation of the antiparallel (a) and parallel (b) magnetic arrangement in trilayered-based systems in the limit ($t_F\gg\ell_{sf}^{(F)}$), ($t_{N1}\ll\ell_{sf}^{(N)}$), and ($t_{N2}\gg\ell_{sf}^{(N)}$). The hatched regions indicate the limits of the extension of the spin accumulation in the magnetic layers at the distance $\ell_{sf}^{(F)}$ from the interface with the central nonmagnetic layer.

## IV. EXPERIMENTAL RESULTS ON *Py*/Cu NANOWIRES WITH CONVENTIONAL STACKING

In our magnetoresistance (MR) measurements on $Py$/Cu with conventional periodic stacking, the linear variation of Eq. (1) is observed only in a narrow thickness range, that is for thin $Py$ layers (a few nm) separated by definitely thicker Cu layers. We see in Fig. 3 that, for multilayers with $t_{Py}=4$ nm, Eq. (1) is obeyed for $t_{\mathrm{Cu}}\geqslant 20$ nm, which appears to be the condition to reduce the dipolar interactions between neighbor layers sufficiently and obtain at the coercive field the random magnetic configuration required by Eq. (1). The fit to the linear variation gives

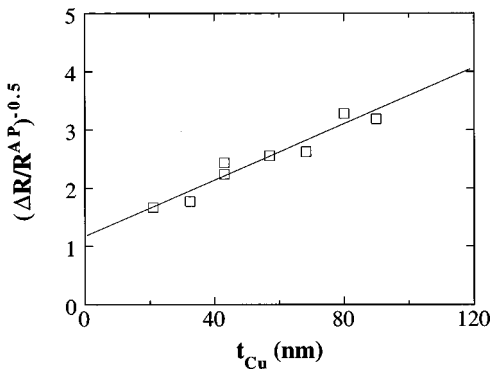


FIG. 3. Plot of $(\Delta R/R^{\mathrm{AP}})^{-1/2}$ vs $t_{\mathrm{Cu}}$ at $T=77$ K for $Py(4\,\mathrm{nm})/\mathrm{Cu}(t_{\mathrm{Cu}})$ multilayered nanowires.

$$\left(\frac{\Delta R}{R^{\mathrm{AP}}}\right)^{-1/2} = a \cdot t_{\mathrm{Cu}} + b$$

with $a = 0.024 \pm 0.002$ and $b = 1.2 \pm 0.1$.

According to Eq. (1), $b$ is necessarily larger than 1 and reaches 1 (that is $\Delta R/R^{\mathrm{AP}} = 1$ or $R^{\mathrm{P}} = 0$) for $\beta = \gamma = 1$. The fact that our experimental value of $b$ is close to 1 suggests values of $\beta$ and $\gamma$ close to 1 but, strictly, the respective values of $\beta$ and $\gamma$ cannot be extracted independently from data with a single value of $t_{Py}$ (or from data with not different enough values of $t_{Py}$), that is from a single set of values of $a$ and $b$. Nevertheless, by allowing the values of $\rho^*_{Py}$, $\rho^*_{\mathrm{Cu}}$, $r^*_{Py}/\mathrm{Cu}$ to vary in reasonable ranges (consistent with previous data on multilayers or nanowires[7,16,18]), we find that both $\beta$ and $\gamma$ have to be between 0.7 and 0.9. This is in agreement with values recently found in $Py/\mathrm{Cu}/Py$ spin valves ($\beta \sim \gamma \sim 0.73$[18]).

It is interesting to compare the results of our group on Co/Cu (Ref. 16) and $Py/\mathrm{Cu}$ nanowires. We find similar values of $\gamma$ ($\gamma = 0.85 \pm 0.1$ for Co/Cu, $0.7 < \gamma < 0.9$ for $Py/\mathrm{Cu}$) but the value of $\beta$ is definitely smaller in Co ($\beta = 0.36 \pm 0.04$) than in *Py* ($0.7 < \beta < 0.9$), which accounts for the higher CPP-GMR we observe in $Py/\mathrm{Cu}$ nanowires. Surprisingly, the GMR is generally larger in Co/Cu than in $Py/\mathrm{Cu}$ in the CIP geometry. It is not clear whether this is due to a weaker influence of bulk scattering in CIP or to structural problems related to the small thicknesses used in the CIP geometry.

In the long SDL limit analyzed above, the GMR does not depend on the SDL. As shown in Refs. 16 and 17, the SDL in Co can be determined simply from conventional multilayers with layer thicknesses satisfying $t_F \gg \ell_{sf}^{(F)}$, $t_N \ll \ell_{sf}^{(N)}$. Unfortunately, as pointed out above and also described in a previous report,[8] with thick *Py* layers and thin Cu layers, the dipolar interactions between layers [attraction between the north and south poles on the two interfaces of thin Cu layers, see Fig. 4(a)] became significant and favors a parallel configuration of successive layers. The probable reversal process is by propagation of reversal from one end of the wire to the other. As a consequence, a relatively small number of interfaces with an antiparallel configuration contributes to the GMR. In other words, the value of the parameter $p$ of Eq. (3) decreases rapidly in the limit of thick *Py* layers and thin Cu layers. It probably explains that, in our GMR measurements on conventional $Py/\mathrm{Cu}$ nanowires, we could not identify a regime where the GMR varies as $1/t_F$. Consequently, we have studied the limit of thick *Py* layers with our second type of structure composed of well separated and noninteracting $Py/\mathrm{Cu}/Py$ trilayers.

## V. EXPERIMENTAL RESULTS ON STRUCTURES COMPOSED OF *Py*/CU/*Py* TRILAYERS SEPARATED BY THICK LAYERS OF Cu

The structure is that represented in Fig. 1(b) and already discussed in Sec. III B. Due to the large separation between the trilayers, one expects dipolar interaction between successive trilayers to become negligeable, each trilayer being almost magnetically isolated. In a given trilayer, as the thickness of the *Py* layers is significantly smaller than the wire diameter, the shape anisotropy favors in plane of the layer magnetization. In addition, at zero field, dipolar interactions

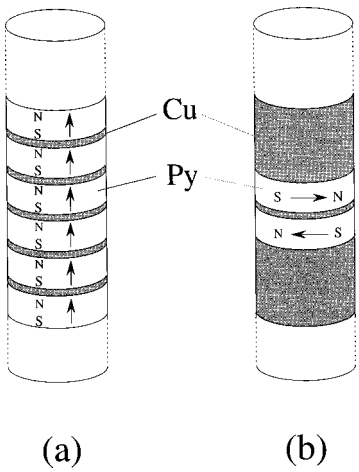


FIG. 4. Sketch of magnetic configurations minimizing the magnetostatic energy for conventional $Py/\mathrm{Cu}$ multilayered nanowires (a) and $Py/\mathrm{Cu}/Py$ trilayers (b) when the Cu layers are thin and the *Py* layers thicker [with $t_{Py}$ < wire diameter in (b)]. In (a), in the configuration with all the magnetizations parallel along the wire axis, the poles separated by thin Cu layers leads to small magnetostatic energy. In the same configuration with parallel magnetizations along the wire for trilayers, the fields generated by the poles on the upper and lower surfaces are not compensated and the magnetostatic energy is high. A smaller energy is obtained with magnetization in the plane of the discs (shape anisotropy of a unique disc) and in opposite directions (as for two magnets laying side by side), as illustrated in (b).

are expected to favor an antiparallel arrangement of magnetic moments in the two successive *Py* layers (discs) of a trilayer, as represented in Fig. 4(b).

The different magnetic behavior of the conventional $Py/\mathrm{Cu}$ multilayers and trilayer systems appear clearly when are compared their magnetization and MR curves. In Fig. 5 we show curves for both structures in the appropriate thickness range for the determination of the spin diffusion length, that is with relatively thick *Py* layers and thin Cu layers. Typical MR curves of antiferromagnetically (AF) coupled and uncoupled Co/Cu planar multilayers are also presented in Figs. 5(c) and (f). The comparison immediately points out the much higher degree of antiparallel (AP) ordering at low field in the trilayer systems.

The two main points are (i) The ratio of the remanent to the saturation magnetization, $M_r/M_s$, is only 12% in the trilayer system of Fig. 5(d) compared to 56% for the multilayer of Fig. 5(a) (the parameter $(1 - M_r/M_s)$ is often taken as a coefficient of AP ordering, equivalent to our parameter $p$, see for example Lenczowski and co-workers[10,25]). Moreover, in the trilayer systems, the ratio $M_r/M_s$ turns out to be practically the same for fields along and perpendicular to the nanowire, which is consistent with an unique zero field arrangement induced by the dipolar forces between the two magnetic layers (discs) of the trilayer [see Fig. 4(b)]. As shown in Fig. 6, the ratio $M_r/M_s$ of trilayer systems remains in the range 10–22% for *Py* thickness up to 100 nm.

(ii) The MR curves are definitely different for the conventional multilayered nanowires and the trilayers systems. In the first case [Fig. 5(b)], the increase of the resistance at $H = 0$ is only a fraction of the maximum increase which is reached at the coercive field. This behavior is reminiscent of

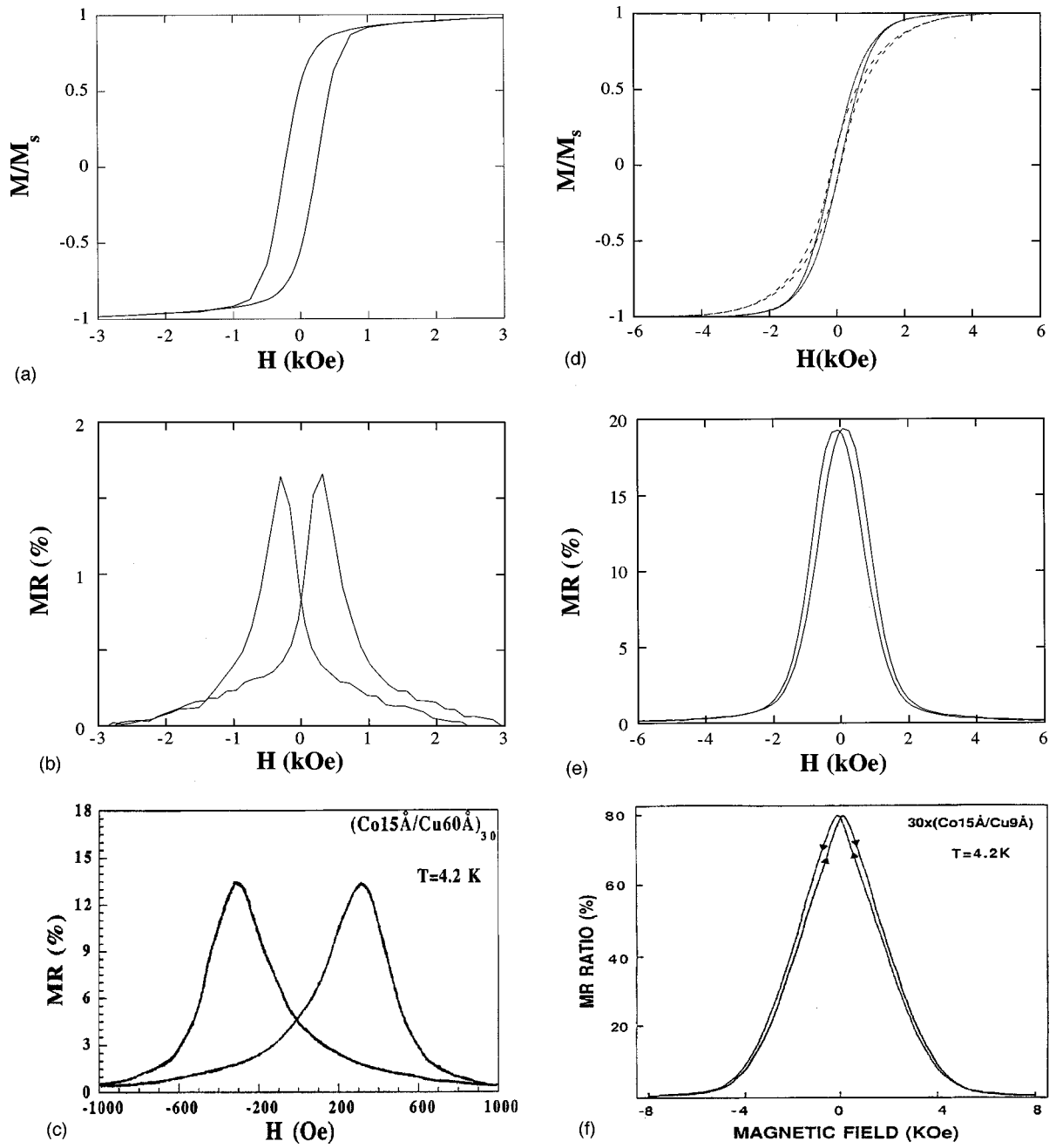


FIG. 5. The magnetization and GMR curves of $Py(60\,\text{nm})/\text{Cu}(15\,\text{nm})$ conventional multilayered nanowires (a), (b) are compared with those of $Py(20\,\text{nm})/\text{Cu}(10\,\text{nm})/Py(20\,\text{nm})$ trilayers separated by 100 nm of Cu [(d), (e); in (d), the full and dashed lines are for fields, respectively, perpendicular and parallel to wire axis]. For comparison, we also show typical GMR curves for uncoupled (Co 1.5 nm/Cu 6 nm) $\times 30$ (c) and AF coupled (Co 1.5 nm/Cu 0.9 nm) $\times 30$ (f) planar multilayers (Ref. 26). The main features are: (i) For conventional Co/Cu nanowires, a large remanent magnetization [$M_r/M_s \sim 0.55$ in (a)] and, in (b), GMR curves similar to those of uncoupled planar multilayers (c) with only a fraction of the GMR reached at $H=0$; (ii) For trilayers systems, a small remanence [$M_r/M_s \sim 0.12$ in both parallel and perpendicular fields in (d)], and, in (e), GMR curves similar to those of AF coupled planar multilayers (f) where the maximum of resistance is reached at $H=0$ in an AF coupled state.

what is observed for the GMR of *uncoupled* planar multilayers, for example at the second and higher order peaks of the MR variation with the Cu thickness in Co/Cu multilayers [Fig. 5(c)].[26] In contrast, for trilayer systems, the MR curves of Fig. 5(e) looks like that at the first peak of antiferromagnetic coupling in Co/Cu planar multilayers [Fig. 5(f)]:[26] the maximum resistance is practically reached at $H=0$ and the two maxima recorded in increasing and decreasing field almost coincide in the close vicinity of $H=0$. This behavior is what is expected when interlayer exchange (in AF coupled planar multilayers) or dipolar forces [between the two magnetic discs of a trilayer of Fig. 4(b)] induce an almost antiparallel configuration at $H=0$.

We conclude from the above discussion of the magnetization and MR curves that a fairly high degree of AP ordering is reached at $H \sim 0$ by the magnetic moments of the two *Py* discs composing a trilayer. From the variation of $(1 - M_r/M_s)$ between 0.78 and 0.9 in Fig. 6, and to take also

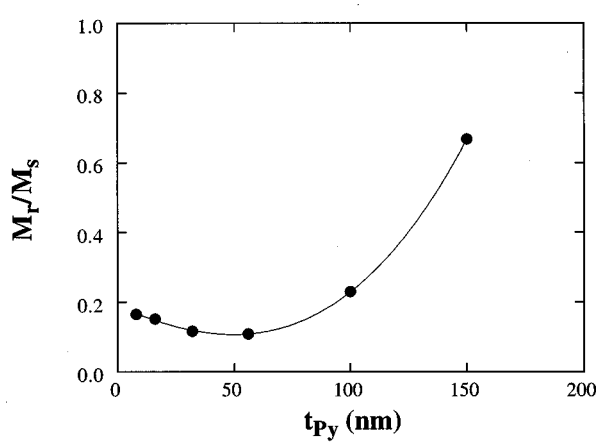


FIG. 6. Remanent magnetization ($M_r/M_s$) as a function of *Py* layer thicknesses in trilayer-based systems. Field is applied parallel to the wire axis. Full line is guide for the eyes.

into account some additional uncertainty in the relation between $(1-M_r/M_s)$ and the parameter $p$ of Eq. (6), we have taken $p=0.85\pm0.15$ for $t_{Py}\leqslant 100$ nm.

The variation of the GMR ratio as a function of the *Py* layer thickness is shown in Fig. 7 for two different trilayer-based systems with $t_{\mathrm{Cu}}=100$ (open circles) and 500 nm (closed squares) for the long Cu rod between trilayers. On increasing the *Py* layer thickness, the GMR goes through a maximum and finally decreases. This variation is, qualitatively, what is expected from Eq. (2). At small values of $t_F$, in the thickness range of the maximum, the MR ratio predicted by Eq. (2) depends on a large number of parameters, not only $\ell_{sf}^{(F)}$ but also $\rho_F^*$, $\beta$, $\rho_N^*$, $r_b^*$, $\gamma$. Our data in the long SDL limit (Sec. IV) did not allow us to determine all these parameters and this makes that there are too many unknown parameters to reliably determine $\ell_{sf}^{(F)}$ from a fit of Eq. (2) with our results in the thickness range of the MR maximum. However, we can see that, for $t_F$ larger than about 20 nm, we reach the regime of Eq. (4) characterized by $\Delta R/R^p$ proportional to $1/t_F$ and independent of $t_{N2}$. In this regime, the only parameters involved in the expression of $\Delta R/R^p$ are $t_F$, $\ell_{sf}^{(F)}$, $p$, and $\beta$. From our analysis of the long

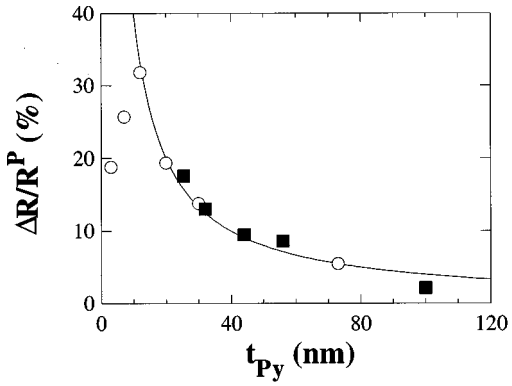


FIG. 7. CPP-GMR vs *Py* layer thicknesses ($t_{Py}$) at $T=77$ K for $Py(t_{Py})$/Cu(10 nm)/$Py(t_{Py})$/Cu(100 nm) (open circles) and $Py(t_{Py})$/Cu(10 nm)/$Py(t_{Py})$/Cu(500 nm) (closed squares) multilayered nanowires. Full line is a fit of experimental data using Eq. (6).

SDL limit, we have derived $\beta=0.8\pm0.1$; this is consistent with the value found by the MSU group, $\beta=0.73\pm0.07$;[18] on the other hand, values of $\beta$ between 0.76 and 0.9 were found in various bulk NiFe alloys.[27] As the value of $\beta$ derived in multilayers is generally somewhat smaller than that determined in bulk alloys, we find that the MSU values, $\beta=0.73\pm0.07$ at the lower limit of our uncertainty range, is more reasonable than 0.8 and we adopted it for our fit of Eq. (4). With, in addition, a reasonable assumption, $0.7<p<1$, for $p$, this leads to

$$\ell_{sf}^{(Py)}=(4.3\pm1.0)\ \text{nm}.$$

The value of the SDL in *Py* is definitely shorter than that found for Co ($\ell_{sf}^{(\mathrm{Co})}=59\pm18$ nm[17]) but, actually, is in good agreement with the SDL of *Py* found by Steenwyk *et al.*[18] from CPP measurements in spin valve structure. We discuss the origin of this short SDL of *Py* in the next section.

## VI. DISCUSSION OF THE SHORT SDL IN *Py*

The most striking result of the present work and also of the recent work of Steenwyk *et al.*[18] is the small value of the SDL in permalloy, $4.3\pm1$ nm in our nanowires, $5.5\pm1$ nm in the spin valve structures of Steenwyk *et al.* Such values are much smaller than in nonmagnetic metals (for example $\ell_{sf}^{(\mathrm{Cu})}=140\pm10$ nm at low temperature in Cu layers[16]) and also definitely smaller than in ferromagnetic Co layers ($\ell_{sf}^{(\mathrm{Co})}=59\pm18$ nm at 77 K[17]). We will, however, show that such a short SDL is expected for permalloy.

We recall the theoretical expression of the SDL of a ferromagnetic layer in the VF model:[11]

$$\left(\frac{1}{\ell_{sf}^{(F)}}\right)^2=\left(\frac{1}{\ell_{\uparrow}}\right)^2+\left(\frac{1}{\ell_{\downarrow}}\right)^2 \tag{5}$$

$$\text{with}\quad \ell_{\uparrow(\downarrow)}=\left[\frac{1}{3}\cdot(v_F\cdot\lambda_{\uparrow(\downarrow)}\cdot\tau_{sf})\right]^{1/2}, \tag{6}$$

where $\lambda_{\uparrow(\downarrow)}$ is the mean free path of the spin $\uparrow(\downarrow)$ electrons and $\tau_{sf}$ is the spin relaxation time (to make the connection with the notation of electron spin resonance, $\tau_{sf}=2T_1$, where $T_1$ is the spin-lattice relaxation time of the electron spin resonance (ESR) theory).

Combining Eqs. (5) and (6) leads to

$$\ell_{sf}^{(F)}=\left(\frac{\lambda_{sf}\cdot\lambda^*}{6}\right)^{1/2} \tag{7}$$

$$\text{with}\quad \left(\frac{1}{\lambda^*}\right)=\frac{1}{2}\cdot\left[\frac{1}{\lambda_{\uparrow}}+\frac{1}{\lambda_{\downarrow}}\right]. \tag{8}$$

It can be pointed out that if, with $\beta$ close to 1, $\lambda_{\uparrow}$ and $\lambda_{\downarrow}$ are very different, $\lambda^*$ is close to the shorter one that can be very short. This is the case for permalloy and partly explains the difference with cobalt where $\beta$ is small and the shorter mean free path not much shorter than the larger ones. More quantitatively, in a free-electron model,

$$\lambda^*\cdot\rho^*=\frac{m\cdot v_F}{n\cdot e^2}, \tag{9}$$

where $n$ is the total number of conduction electrons (spin $\uparrow$ and spin $\downarrow$) and $v_F$ is the Fermi velocity. A straightforward calculation with one electron per atom ($s$ band), $\rho^*_{Py} = 26.3\,\mu\Omega\,\mathrm{cm}$ [from $\rho^*_{Py} = \rho_{Py}/(1-\beta^2)$ with $\rho_{Py} = 12.3\,\mu\Omega\,\mathrm{cm}$, $\beta = 0.73$ (Ref. 18)] leads to

$$\lambda^* \sim 2.4 \text{ nm}.$$

The spin relaxation time $\tau_{sf}$ is controlled by the spin orbit part of the scattering. In first approximation, we have assumed that the scattering in *Py* at 4.2 K is essentially that of Fe impurities in Ni and that the ratio of the spin-flip scattering to the non-spin-flip scattering has the same value as for Fe impurities in Cu, i.e., $r = 1.125 \times 10^{-2}$,[28] and we find

$$\lambda_{sf} \sim \frac{\lambda^*}{r} = 212 \text{ nm}$$

and, from Eq. (9),

$$\ell_{sf}^{(\mathrm{cal})} \sim 9.2 \text{ nm}.$$

This value is about twice the experimental one, but it is satisfying to find the right order of magnitude. A similar calculation for Co, with $\rho^*_{\mathrm{Co}} = 6.6\,\mu\Omega\,\mathrm{cm}$ (Ref. 29) and $r = 1.2 \times 10^{-2}$ as estimated for Co impurities in Cu (Ref. 28) leads to $\ell_{sf}^{(\mathrm{Co})} \sim 36\,\mathrm{nm}$.

The shorteness of the SDL in *Py* has other implications than in the problems of the CPP-GMR, since it is also an important parameter for the spin switch introduced by Johnson[15] and other devices based on spin injection effects. Our finding of a very short SDL for *Py* gives an additional support to the remark of Steenwyk *et al.*[18] that the very short SDL of *Py* introduced into models[30,31] of the spin switch ''gives a prediction that disagrees with Johnson data.''

## VII. CONCLUSIONS

We have measured the CPP-GMR of extensive series of *Py*/Cu multilayered nanowires, in both the long SDL regime and the regime where, for *Py* layer thicker than the SDL of *Py*, the MR ratio is proportional to the ratio $\ell_{sf}^{(Py)}/t_{Py}$. Two important results are derived from the analysis of our experimental data in the VF model:[11] (a) Both the bulk and interface scattering spin asymmetry coefficient, $\beta$ and $\gamma$, are large in *Py*: $0.7 < \beta$, $\gamma < 0.9$; (b) The SDL in the *Py* layers, $\ell_{sf}^{(Py)} = 4.3 \pm 1$ nm, is much shorter than in cobalt or in noble metals.

Both results are in good agreement with recent findings by Steenwyk *et al.*[18] from measurements on spin valves, i.e., $\beta = 0.73$, $\gamma = 0.7$, $\ell_{sf}^{(Py)} = 5.5 \pm 1$ nm. The large value of $\beta$, larger than in Co [$\beta = 0.36 \pm 0.04$ (Ref. 16)] confirms that the contribution from bulk scattering is important in *Py*-based multilayers and, in fact, explains the large MR effects we observe in *Py*/Cu compared to Co/Cu. More quantitatively, by comparing the interface and bulk additive contributions to the square root of the MR ratio in the inverse of Eq. (1), we find that the interface contribution is larger for *Py* layer thinner than 3.6 nm, while the bulk contribution is predominant for thicker layers.

The very short SDL we find in *Py*, in agreement with a previous similar result by Steenwyk *et al.*,[18] is not surprising. An approximate calculation of the SDL in *Py*, based on the spin-flip cross section of Fe impurities determined by ESR, leads to a value of the SDL of the same order of magnitude, much shorter than in cobalt and noble metals.

## ACKNOWLEDGMENTS

We thank the Unité de Physique et de Chimie des Hauts Polymères (UCL) for providing the polycarbonate membrane samples used in this study. L.P. thanks the National Fund for Scientific Research (Belgium) for support. This work has been partly supported by a Brite program of the European Commission (BE95-1761) and by the Belgian Interuniversity Attraction Pole Program (PAI-IUAP P4/10).

[1] L. Piraux, J. M. George, J. F. Despres, C. Leroy, E. Ferain, R. Legras, K. Ounadjela, and A. Fert, Appl. Phys. Lett. **65**, 2484 (1994).

[2] A. Blondel, J. P. Meir, B. Doudin, and J.-Ph. Ansermet, Appl. Phys. Lett. **65**, 3019 (1994).

[3] K. Liu, K. Nagodawithana, P. C. Pearson, and C. L. Chien, Phys. Rev. B **51**, 7381 (1995).

[4] W. P. Pratt, S. F. Lee, J. M. Slaughter, R. Loloee, P. A. Schroeder, and J. Bass, Phys. Rev. Lett. **66**, 3060 (1991).

[5] M. A. Gijs, S. K. J. Lenczowski, and J. B. Giesbers, Phys. Rev. Lett. **70**, 3343 (1993).

[6] W. Vavra, S. F. Cheng, A. Fink, J. J. Krebs, and G. A. Prinz, Appl. Phys. Lett. **66**, 2579 (1995).

[7] S. F. Lee, W. P. Pratt, Q. Yang, P. Holody, R. Loloee, P. A. Schroeder, and J. Bass, J. Magn. Magn. Mater. **118**, 1 (1993); W. P. Pratt, S. F. Lee, P. Holody, Q. Yang, R. Loloee, J. Bass, and P. A. Schroeder, *ibid.* **126**, 406 (1993); Q. Yang, P. Holody, S. F. Lee, L. L. Henry, R. Loloee, P. A. Schroeder, W. P. Pratt, and J. Bass, Phys. Rev. Lett. **72**, 3274 (1994).

[8] S. Dubois, C. Marchal, J. M. Beuken, L. Piraux, J. L. Duvail, A. Fert, J. M. George, and J. L. Maurice, Appl. Phys. Lett. **70**, 396 (1997).

[9] S. S. P. Parkin, Appl. Phys. Lett. **60**, 512 (1992).

[10] S. K. J. Lenczowski, M. A. M. Gijs, R. J. M. Van De Veerdonk, J. B. Giesbers, and W. J. M. de Jonge, in *Magnetic Ultrathin Films, Multilayers and Surfaces*, edited by A. Fert, H. Fujimori, G. Guntherodt, B. Heinrich, W. F. Egelhoff, Jr., E. E. Marinero, and R. L. White, MRS Symposia Proceedings No. 384 (Materials Research Society, Pittsburgh, 1995), p. 341.

[11] T. Valet and A. Fert, Phys. Rev. B **48**, 7099 (1993).

[12] S. F. Lee, W. P. Pratt, R. Loloee, P. A. Schroeder, and J. Bass, Phys. Rev. B **46**, 548 (1992).

[13] B. Voegeli, A. Blondel, B. Doudin, and J. Ph. Ansermet, J. Magn. Magn. Mater. **151**, 388 (1995).

[14] L. Piraux, S. Dubois, C. Marchal, J. M. Beuken, L. Filipozzi, J. F. Despres, K. Ounadjela, and A. Fert, J. Magn. Magn. Mater. **156**, 317 (1996).

[15] M. Johnson, Phys. Rev. Lett. **70**, 2142 (1993).

[16] L. Piraux, S. Dubois, and A. Fert, J. Magn. Magn. Mater. **159**, L287 (1996).
[17] L. Piraux, S. Dubois, A. Fert, and L. Beliard, Eur. Phys. J. B **4**, 413 (1998).
[18] S. D. Steenwyk, S. Y. Hsu, R. Loloee, J. Bass, and W. P. Pratt, J. Magn. Magn. Mater. **170**, L1 (1997); W. P. Pratt, S. D. Steenwyk, S. Y. Hsu, W. C. Chiang, A. C. Schaefer, R. Loloee, and J. Bass, IEEE Trans. Magn. **33**, 3505 (1997).
[19] E. Ferain and R. Legras, Nucl. Instrum. Methods Phys. Res. B **131**, 97 (1997), and references therein.
[20] R. Ferré, K. Ounadjela, J. M. George, L. Piraux, and S. Dubois, Phys. Rev. B **56**, 14 066 (1997).
[21] J. L. Maurice, D. Imhoff, P. Etienne, O. Durand, S. Dubois, L. Piraux, J. M. George, P. Galtier, and A. Fert, J. Magn. Magn. Mater. **184**, 1 (1998).
[22] A. Fert, J. L. Duvail, and T. Valet, Phys. Rev. B **52**, 6513 (1995).
[23] S. Y. Hsu, A. Barthélémy, P. Holody, R. Loloee, P. A. Schroeder, and A. Fert, Phys. Rev. Lett. **78**, 2652 (1997).
[24] S. Zhang and P. M. Levy, Phys. Rev. B **47**, 6776 (1993).
[25] S.K.J. Lenczowski, M.A.M. Gijs, R.J.M. Van de Veerdonk, J.B. Giesbers, and W.J.M. de Jonge, in *Magnetic Ultrathin Films, Multilayers and Surfaces* (Ref. 10); S. Lenczowski, M. Gijs, J. Giesbers, R. van de Veerdonk, and W. de Jonge, Phys. Rev. B **50**, 9982 (1994).
[26] D. H. Mosca, F. Petroff, A. Fert, P. A. Schroeder, W. P. Pratt, and R. Loloee, J. Magn. Magn. Mater. **94**, 1 (1991); F. Petroff, Ph.D. thesis, Orsay, France, 1992.
[27] I. A. Campbell and A. Fert, in *Ferromagnetic Materials*, edited by E. P. Wohlforth (North-Holland, Amsterdam, 1982).
[28] P. Monod and S. Schultz, J. Phys. (France) **43**, 393 (1982).
[29] J. Bass, W. P. Pratt, Jr., and P. A. Schroeder, Comments Condens. Matter Phys. (to be published).
[30] A. Fert and S. F. Lee, Phys. Rev. B **53**, 6554 (1996); J. Magn. Magn. Mater. **165**, 115 (1997).
[31] S. Hershfield and H. L. Zhao, Phys. Rev. B **56**, 3296 (1997).